JTTEE5 17:685–691
DOI: 10.1007/s11666-008-9259-0
1059-9630/$19.00 © ASM International

Effective Parameters in Axial Injection Suspension Plasma Spray Process of Alumina-Zirconia Ceramics

F. Tarasi, M. Medraj, A. Dolatabadi, J. Oberste-Berghaus, and C. Moreau

(Submitted May 13, 2008; in revised form September 19, 2008)

Suspension plasma spray (SPS) is a novel process for producing nano-structured coatings with metastable phases using significantly smaller particles as compared to conventional thermal spraying. Considering the complexity of the system there is an extensive need to better understand the relationship between plasma spray conditions and resulting coating microstructure and defects. In this study, an alumina/8 wt.% yttria-stabilized zirconia was deposited by axial injection SPS process. The effects of principal deposition parameters on the microstructural features are evaluated using the Taguchi design of experiment. The microstructural features include microcracks, porosities, and deposition rate. To better understand the role of the spray parameters, in-flight particle characteristics, i.e., temperature and velocity were also measured. The role of the porosity in this multicomponent structure is studied as well. The results indicate that thermal diffusivity of the coatings, an important property for potential thermal barrier applications, is barely affected by the changes in porosity content.

Keywords alumina-yttria stabilized zirconia, effective parameters, nanocomposite, suspension plasma spray

1. Introduction

Suspension plasma spray (SPS) is an emerging process for spraying small feedstock particles with nano and/or a few micron size ranges, using a liquid carrier. These particles are mostly less than 5 μm in dimension and are difficult to feed using conventional equipment, since they tend to form larger aggregates that can cause blocking of the injection path. Injection of such particles into a plasma jet can be achieved with the help of liquid carriers. The resulting microstructure favors dense or finely porous structures as needed for solid oxide fuel cell electrolytes (Ref 1) or cathodes (Ref 2). However, more investigation is required for better controlling the range of porosity and other structural features obtainable with this process. SPS can generate unique and novel microstructure, not commonly seen in conventional thermal spraying (Ref 3) and understanding the role of the process parameters, which impart these microstructural features, has increasing importance.

In addition, the feedstock size and size distribution as well as the nature of the material play important roles. Using multicomponent feed materials increases the difficulty of producing uniform microstructures in the coatings, for example, mixtures of alumina and yttria-stabilized zirconia (YSZ). One reason is the effect of combination of the molten particle and substrate material on splat shape and morphology (Ref 4) that may continue in the following layers with alternating material (e.g., alumina or zirconia layers of the composite coating) and results in unexpected splat behavior as compared with a substrate of a single material. Meanwhile, substrate roughness is another important process parameter in the coating studies.

This study was conducted to identify the significant process parameters, involving the plasma torch, feed, and substrate in producing a sound and integrated microstructure. Such a structure is required for further studies of the characteristic properties of the coatings produced by the SPS process. The eutectic composition of alumina/8 wt.% YSZ was used in this study.

2. Experimental

2.1 Liquid Feed Material

To produce two different powder size ranges, 5 wt.% YSZ and 13 wt.% YSZ (Nano-Composite Powder, Inframat@Advanced Materials; Farmington, USA, size

This article is an invited paper selected from presentations at the 2008 International Thermal Spray Conference and has been expanded from the original presentation. It is simultaneously published in *Thermal Spray Crossing Borders, Proceedings of the 2008 International Thermal Spray Conference*, Maastricht, The Netherlands, June 2-4, 2008, Basil R. Marple, Margaret M. Hyland, Yuk-Chiu Lau, Chang-Jiu Li, Rogerio S. Lima, and Ghislain Montavon, Ed., ASM International, Materials Park, OH, 2008.

F. Tarasi, M. Medraj and **A. Dolatabadi**, Industrial and Mechanical Engineering Department, Concordia University, Sir George Williams Campus, 1515 St. Catherine W., Montreal, QC, Canada H3G 2W1; and **J. Oberste-Berghaus** and **C. Moreau**, NRC-IMI, Boucherville, QC, Canada. Contact e-mail: mmedraj@me.concordia.ca.

30-60 nm) nano-powders were proportionally mixed to produce 8 wt.% YSZ, which is the common thermal barrier coating (TBC) material in gas turbines and diesel engines. The resulting doped zirconia powders were then mixed with two different sizes of alumina powders. The alumina component was either nano size (Nanostructured & Amorphous Materials Inc. USA, Nominal size 27-43 nm) or micron size (Malakoff, TX, size 1.4 μm). The terms ''Nano'' and ''Micron,'' respectively, will be used here for these mixtures. The mixture with the larger size powder was ball milled in a concentrated suspension of 60 wt.% solid for 24 h before dilution to the final solid concentration. This procedure ensured homogeneous mixing and stabilization of the suspension. The nano mixture was only milled for the same period for enhanced stability of the suspension. A weight ratio of 60/40 for the alumina/8 wt.% YSZ were prepared and suspended in ethanol at 10 and 30 wt.% concentrations. This resulted in four suspensions with different powder size ranges and solid contents. Suspension dispersion was done using 9 cc (poly-ethylene-imine) and 4.5 cc (nitric acid) (both with 10% concentration) for every 150 g of solids. Wet analysis of the suspension was performed by infrared Culter-Beckman particle size analyzer to determine the size of agglomerated solid particles in the suspension.

2.2 Methodology

The Mettech Axial III spray system (Northwest Mettech, North Vancouver, Canada) was used. This torch consists of three cathodes and three anodes that can reduce the average arc voltage fluctuations. The injection system is fully automated and PC controlled to ensure a constant feed rate, which can have significant effects on the spray process and the resulting coatings. The spray distance was kept constant at 50 mm, as short spray distances are commonly used in SPS (Ref 5, 6). In-flight particle characteristics (velocity and temperature) were monitored by the diagnostic system Accura-Spray G2 (Tecnar Automation, St. Bruno, Canada). This system measures particle temperature and velocity based on particle ensemble signals rather than the signal from individual particles. The measurements were taken at the substrate position.

Field emission scanning electron microscope FE-SEM (Hitachi S4700) was used to image the coating microstructure. Whereas SEM (Jeol JSM-610) was utilized in image analysis (IA) at 500× magnification and the average porosity was determined from measurements in 10 locations. Calibrations of brightness and contrast were selected between two reference materials, namely aluminum foil and the mounting material. This method is useful for large porosities in the coating; and is limited to the detection of the pores greater than 0.5 μm (Ref 7).

The vertical and horizontal cracks that are sometimes reported as a part of total porosity were individually assessed and counted per unit length or width of the coating. Five measurements were averaged per sample. The nature of the cracks can have significant influence on the properties of the coating. For example, it was observed that the planar defects parallel to the substrate are more influential on mechanical properties (Ref 8) as well as thermal diffusivity (Ref 8, 9), than the total porosity. Vickers microhardness test using 300 g loads for 15 s was done on selected samples. Thermal diffusivity was evaluated by the laser flash method (Ref 10).

The statistical method of Taguchi was used to evaluate the importance of seven selected variables in the SPS coating process, including feed, plasma torch condition, and substrate-related variables. The need to investigate a wide range of variables with the minimum number of experimental runs provoked the application of this design of experiment (Ref 11). The variables and their two selected levels are summarized in Table 1. Among the variables in Table 1, the levels for solid content, torch condition, and feed rate were selected based on the initial data from the equipment supplier, followed by the preliminary trial and errors by the authors for the favorable working condition. Additionally, the substrate roughness was in the range of what is used in the industry and the robot speed was changed from the medium to the maximum attainable speeds by the spray robot.

The microstructural features and in-flight particle characteristics on which the effects of variables are being studied were:

- Particle temperature, T_p, at impact distance (°C).
- Particle velocity at impact distance, V_p (m/s).
- Vertical cracks average spacing (μm).
- Horizontal cracks average spacing (μm).
- Porosity content in the crack-free area (%).
- Thickness per pass of deposition or deposition rate (μm/pass).

3. Results and Discussions

3.1 Suspension Agglomerate Size Distribution

The wet analyses of the agglomerate size in different suspensions diluted in ethanol were closely comparable

Table 1 Variables and their levels (values)

Variable		Low & high levels
A	Solid content in suspension	10 & 30 wt.%
B	Auxiliary gas	H_2 and He
C	Torch condition (total plasma gas flow, gas composition, torch current)	(245 slm, 75Ar/10N_2/15 auxiliary gas, 200 A) & (275 slm, 65Ar/15N_2/20 auxiliary gas, 240 A)
D	Injected feed rate	1.3 & 1.8 kg/h
E	Powder type	Nano & Micron
F	Substrate roughness	#24 & #60 mesh size of alumina for grit blasting
G	Spraying robot travel speed	0.6 & 2 m/s

regardless of the initial particle size or solid concentrations and are all in the range of 10 μm. That is, 0.2-3 μm in 30% solid of micron-sized particle suspension, 0.2-9 μm in 10% solid of the same powder, and 0.2-5 μm in nano-sized powder in 10% solid suspension.

3.2 Effects of the Variables

A summary of the results of the Taguchi evaluations are shown in bar chart graphs in Fig. 1. The first column for every variable shows the effect of its variation from the low level to high level as defined in Table 1. The second column for each variable is the standard error to help comparison of the significance of the effects with the error.

When changing the variable (e.g., solid weight%) from low to high level increases the specific structural parameter (e.g., vertical crack spacing) in the coating, the related column is shown on the positive side of the Y-axis and the decreasing effects of variables on the measured parameter are shown on the negative side of this axis.

By relating the particle temperature and velocity to the spray conditions, some general trends can be observed and will be discussed in the following sections.

3.2.1 Solid Concentration. Increasing the solid content from 10 to 30% in the suspension liquid, as observed in Fig. 1(a) and (b), has decreased both particle temperature and velocity. The coatings from this lower temperature and velocity have shown no considerable change in vertical crack density, but the spacing of horizontal cracks through the thickness increased slightly as presented in the diagrams of Fig. 1(c) and (d). Within the precision of the method used in these experiments the porosity content of the coatings was not affected by the solid concentration. It, however, shows to be the most effective factor on deposition rate, as shown in Fig. 1(e) and (f). The higher solid content in the liquid feed has produced thicker layers per pass, which can be translated to the higher rate of material deposition. It can also be reasoned that thicker splats are a result of lower T_p, causing higher droplet viscosity, and lower V_p, causing lower momentum for deformation, both of which could reduce the splat flattening.

3.2.2 Plasma Auxiliary Gas. Changing the plasma auxiliary gas from commonly used hydrogen to helium, was implemented to induce more porous microstructures for applications like thermal barrier coatings. Helium is

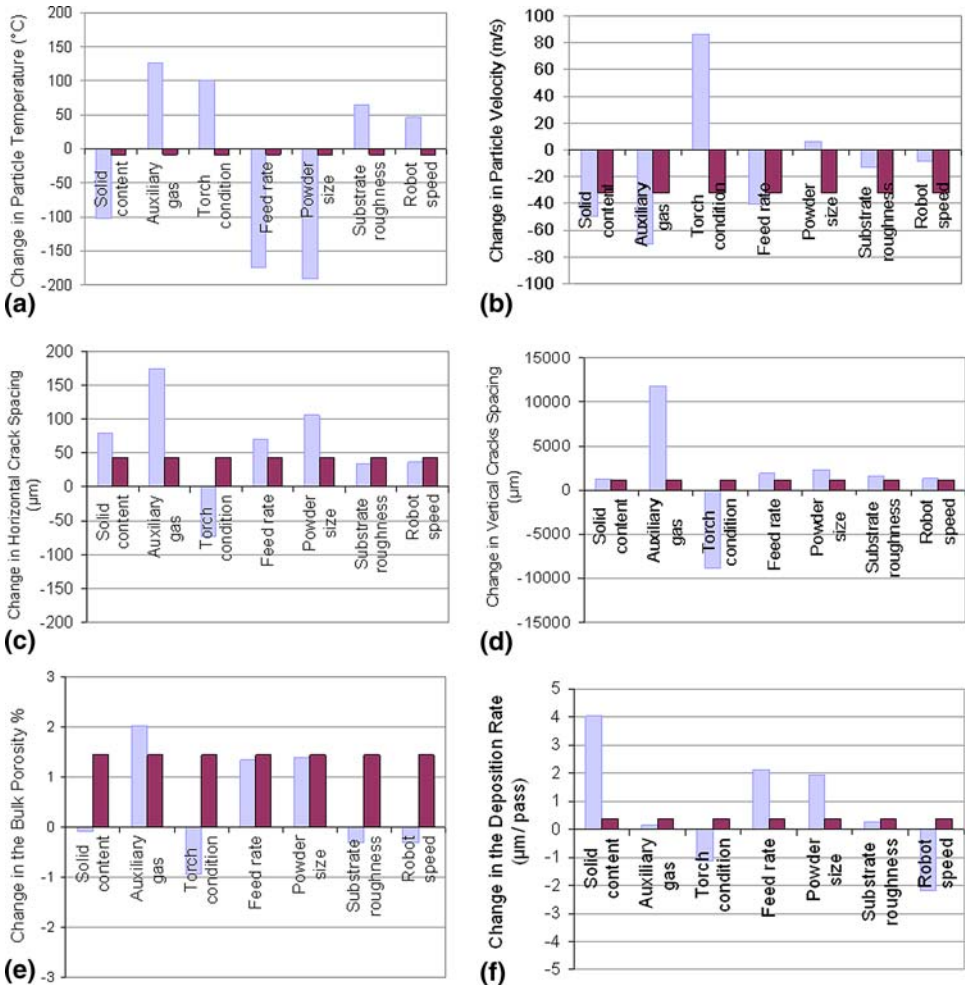

Fig. 1 The averaged effects of the seven variables on particle characteristics and microstructural parameters in SPS process

known to increase the plasma stability with its higher viscosity at high temperature [5]. It also has a higher conductivity than Argon and generally produces wider hot core area that promotes entrapment of larger number of small particles, which could otherwise escape from the particle jet without deposition. The observed effects of this change are summarized in Fig. 1(a) to (f).

Interestingly, changing from hydrogen to helium auxiliary gas has shown the most drastic effect on almost all of the measured parameters in this work. This experiment using the Taguchi method has shown that by replacing H_2 with He gas, the average particle temperature increases and the average velocity decreases. One by one comparison, however, gives some more information that may be extracted from Fig. 2. This figure shows that at the same plasma torch condition (in terms of total gas flow rate, plasma gases ratio, and arc current), He has dropped the resulting plasma power by 20-40 kW. This can be observed in two different plasma conditions of "245 slm total gas flow rate, 75Ar/10N_2/15 auxiliary gas, 200 A current" and "275 slm total gas flow rate, 65Ar/15N_2/20 auxiliary gas, 240 A current."

On the other hand, comparison between the two sets of experiments in Fig. 2 clearly shows that He auxiliary gas resulted in both higher velocity and temperature of the in-flight particles, even though only small differences of plasma power around 80-82 and 84-85 kW were recorded. This temperature increase, in spite of shorter heat exposure time at higher velocity, is a result of higher heat conduction by helium gas.

The SPS coatings produced within the range of variables in this experiment show a very dense microstructure. The porosity in crack-free areas ranges from a minimum of almost zero, produced with hydrogen auxiliary gas, to a maximum of 8% with helium. The two extreme microstructures of alumina/YSZ coatings are shown in the micrographs of Fig. 3(a) and (b). It is clear that while the high density of the coating in Fig. 3(c) causes the vertical microcracks to develop within the structure, the porous structure, especially in the case of distributed porosities as in Fig. 3(d), eliminates the microcracks. A comparison of the particle temperatures and velocities indicated on the micrographs as (T_p, V_p) shows that for high densities a high particle velocity is necessary.

3.2.3 Plasma Torch Condition. Changing the plasma condition from the low to high level, as described in Table 1 and based on the results in Fig. 1(a) and (b), raised the particle temperature and, to an even higher degree, the particle velocity. At higher particle temperature and velocity the density of both vertical and horizontal cracks increases. This may originate from formation of thinner splats that can more readily form vertical cracks during the cooling process. The horizontal cracks branch from the vertical cracks. In this way, the similar behavior from both types of cracks may also be justified. The porosity remains invariant and the deposition rate decreases slightly. A direct comparison, however, is difficult since the parameters of spray torch condition and auxiliary gas are not independent. To gain further insight into the effect of plasma power, deposition runs can be grouped into four ranges of plasma power of 56-57, 80-82, 84-85, and 116-118 kW. Accordingly, the effect of different plasma input powers on the particle characteristics is summarized in Fig. 4. It can be seen that an increase in plasma power generally increases the particle velocity. At similar plasma power (81-84 kW), particle velocity in

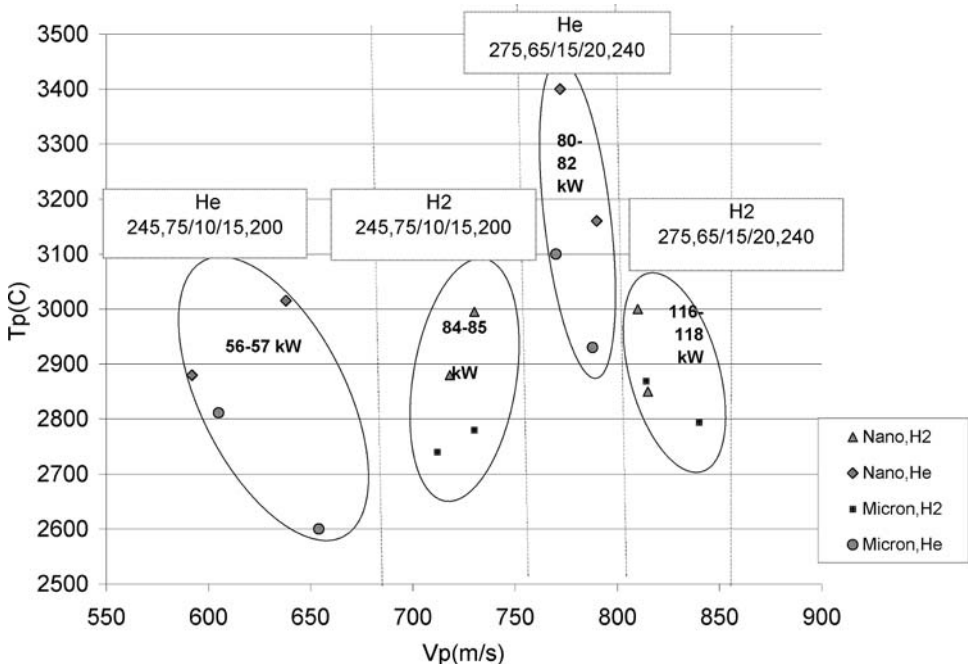

Fig. 2 The effect of auxiliary gas, powder size, torch condition, and plasma power on particle velocity and temperature

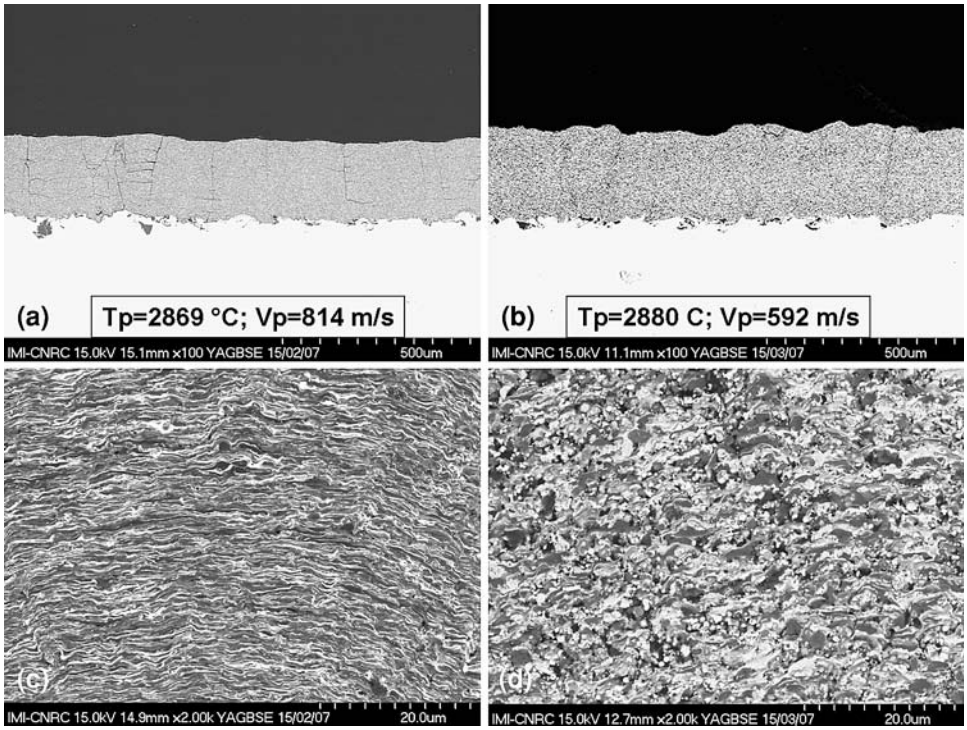

Fig. 3 60/40 wt.% alumina/zirconia suspension plasma-sprayed coatings (a, b) coatings at 100×. (c, d) Same coatings as (a, b), respectively at 2000×

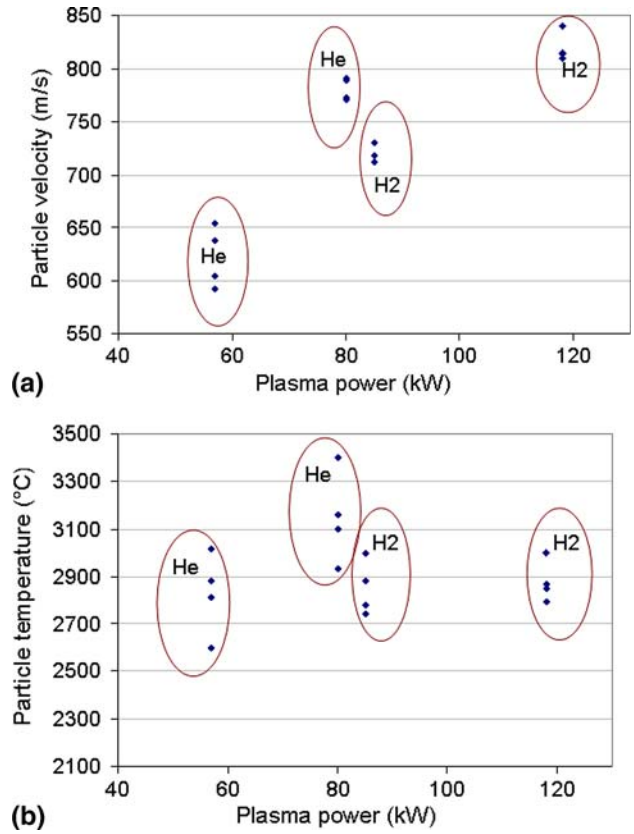

Fig. 4 Plasma power effect on (a) particle velocity and (b) particle temperature

helium exceeds that in hydrogen as shown in Fig. 4(a). Nonetheless, the highest particle velocities are attained with hydrogen.

As a result of the above condition, the average porosity increased with helium and both vertical and horizontal cracks spacing show an increasing trend presented in Fig. 1(c) to (f). Moreover, Fig. 1(e) shows that the deposition rate was indifferent to this change. The temperature of the particles, however, does not follow a definitive trend, as seen in Fig. 4(b). Generally, it was observed that the feed parameters are better tools for controlling the particle temperature than the torch operating parameters.

3.2.4 Feed Rate. Based on the Taguchi analysis in Fig. 1(a) to (d), increasing feed rate decreases both particle temperature and to a lesser extent particle velocity. As a result, the microcracks densities do not show any considerable variation. The porosity also did not get affected by this change, as represented in Fig. 1(e). Conversely, the deposition rate, shown in Fig. 1(f), increases remarkably. This characteristic of the process that can tolerate the increase of the feed rate and deposition rate without introducing more structural defects in the coating is promising for higher production rates.

It is noteworthy that the feed rate and the solid content have shown similar effects and may be interchangeably used in controlling the coating microstructure in the SPS process.

3.2.5 Powder Size Distribution. The change in the initial particle size range was done by changing nano- to micron-size alumina powders mixed with nano-size 8 wt.% YSZ.

This variation showed a recurring drop in particle temperature (T_p) in spite of the similar agglomerate size in the suspension; and no significant velocity drop occurred. The lower temperature from larger particle feedstock may be explained by the formation of dense particles within the plasma plume in comparison with hollow particles, which can result from nano-size suspension feedstock (Ref 12). A second reason for higher (T_p) can be that the nano particles that form loose aggregates are of considerably higher surface area thus showing lower energy barrier for melting than solid micron-sized particles in the aggregates. Experiencing the same velocity and spray distance, the nano aggregates, more rapidly melted, can rise to higher temperatures.

In the resulting coating microstructure the average porosity presented no change and while the density of vertical microcracks remained almost constant and the horizontal microcrack spacing increased remarkably. The lower microcrack densities observed with larger particles can also be justified by the lower T_p as the high particle temperatures can cause higher thermal stresses. The porosity content looks indifferent to the powder size variation. This is somewhat unexpected. Considering the large standard error, a possible underlying effect may not be captured. The limited sensitivity of the porosity measurement method also has restricted the observation of the smaller pores (nano-pores) that might have affected the results.

3.2.6 Substrate Roughness. Keeping in mind that the substrate roughness has no effect on in-flight particle characteristics, this experiment shows that its variation is one of the least effective parameters on the microstructural features, as seen in Fig. 1. Neither the porosity nor the deposition rate has changed, and even the microcrack densities (vertical/horizontal) have not been considerably altered by changing the substrate roughness taking into account the standard error in these measurements.

Additionally, the averages of coating roughness on the substrates blasted with #60 alumina grit ($R_a = 3\text{-}4$ μm) and #24 grit ($R_a = 6\text{-}7$ μm) substrates are almost the same, namely $R_a = 5.5$ and 6 μm, respectively. The absence of strict correlation between the initial substrate roughness and the resulting coatings is attributed to the small aggregate sizes comparable with the size of substrate roughness. The small particles at high velocity diffuse into the roughness asperities and after the first few runs of deposition eliminate the role of the substrate roughness. This independency of the roughness between the substrate and coating suggests that the coating roughness can be controlled by spray condition for various substrate roughnesses. On the other hand, changing the initial particle size from nano to micron-size powders causes a slightly more considerable effect on coating roughness, namely, from $R_a = 5.1$ to 6.3 μm.

3.2.7 Robot Travel Speed. Increasing the robot travel speed, again not having any effect on particle state, has neither changed the porosity nor the vertical/horizontal microcracks density. A drop in deposition rate is simply related to less mass deposition time at higher robot travel speed.

3.3 Particle Velocity, Porosity, and Hardness

A demonstration of the effect of particle velocity on the coating density indicated in Fig. 5(a) shows that coating density increases as a result of higher particle velocity that provides higher momentum for the splat flattening, as is expected. This also has resulted in enhanced intersplat bounding that has clearly improved the hardness of the resulting coating as illustrated in Fig. 5(b). This figure shows that with even less than 5% porosity, the coating hardness drops to less than one third of the highly dense structure.

3.4 Porosity and Thermal Diffusivity

A group of samples with a range of porosities ranging from the minimum to the maximum were evaluated for thermal diffusivity. The results are summarized in Fig. 6. A porosity of 0-8% in the crack-free area obtained in this experience has not altered the thermal diffusivity of the coating. The measured thermal diffusivities of the coatings are, however, comparable with that of the stabilized zirconia sprayed with the same process. It is noteworthy that the thermal conductivity of the 8 wt.% YSZ formed by this process was measured as 0.89 W/m °C. This value is in turn comparable to values reported in the literature (Ref 13) for air plasma-sprayed YSZ (0.9-1 W/m °C) and YSZ deposited by EB-PVD (Electron beam physical vapor deposition) in the order of 1.8-2 W/m °C.

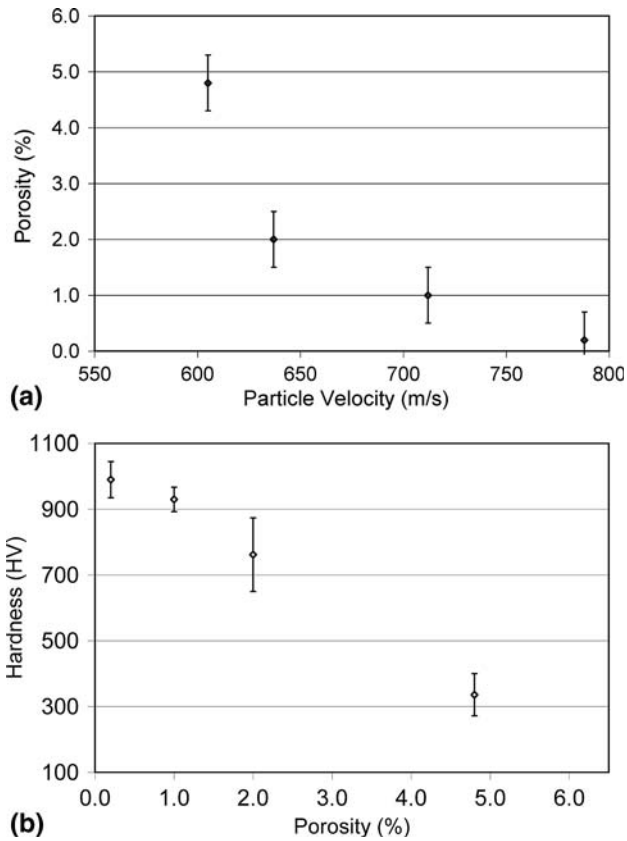

Fig. 5 The variation of the coating porosity versus particle velocity (a) and the coating hardness versus coating porosity (b)

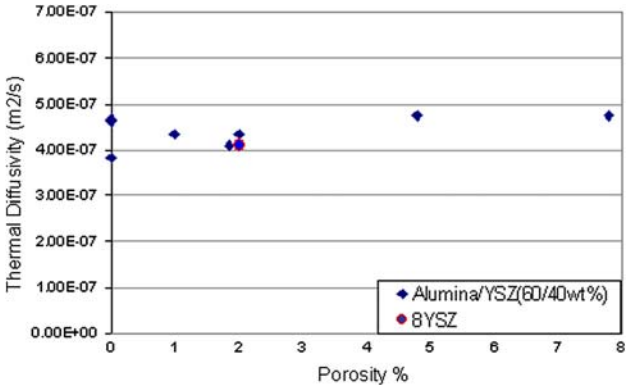

Fig. 6 The variation of thermal diffusivity with the porosity content

These results suggest that porosity may not be the most significant factor for thermal barrier applications. In this way the implementation of dense composite coating can promote the potentially better mechanical properties. It should be considered, in the thermal diffusivity versus porosity results, that the smaller pores of submicron sizes could not be detected in the image analysis method with magnification as low as 500×. However, it is proven that the roles of size, shape, and densities of the intersplat pores in thermal diffusivity are more important than the total porosity content (Ref 14).

4. Summary and Conclusion

In this study, the importance of some key variables in suspension plasma spraying of multicomponent alumina/stabilized zirconia coatings was evaluated.

It was observed that the variables that directly affect the particle velocity and temperature were the most influential on the microstructure. Considering the greater significance of particle velocity in this regard, variables with more prominent effect on V_p were of prime importance. The substrate and robot-related variables that do not play a role on any of T_p or V_p did not consequently affect the coating microstructure.

It was noticed that the plasma torch parameters, e.g., total gas flow rate and plasma gas composition, were most important in varying the particle velocity. On the other hand, particle temperature is more readily manipulated by feed stock parameters like solid content, particle size, and feed rate.

Helium auxiliary gas was successfully used as a tool to achieve a wider microstructural variety in the SPS coatings. It especially helped in increasing the porosity content in the coating. The porosity, however, increased at the expense of reducing the coating hardness.

Thermal diffusivity in SPS coatings for a multicomponent system of 60alumina/40YSZ is reasonably low and does not change with bulk porosity of up to 8%.

References

1. C. Delbos, C. Rat, C. Bonhomme, J. Fazilleau, J.F. Coudert, and P. Fauchais, Influence of Powder Size Distributions on Microstructural Features of Finely Structured Plasma Sprayed Coatings, *High Temp. Mater. Process.*, 2004, **8**, p 397-406
2. C. Monterrubio-Badillo, H. Ageorges, T. Hartier, J.F. Codert, and P. Fauchais, Plasma Spraying of a Perovskite Suspension for SOFC Cathodes, *Proceedings of the 2003 International Thermal Spray Conference: Advancing the Science & Applying the Technology*, B.R. Marple and C. Moreau, Eds., May 5-8, 2003 (Orlando, FL), ASM International, 2003, p 687-692
3. S. Siegmann, N. Margadant, A. Zagorski, and M. Arana-Antelo, Composition of Particle In-Flight-Characteristics and Coating Properties, *Proceedings of the 2003 International Thermal Spray Conference: Advancing the Science & Applying the Technology*, B.R. Marple and C. Moreau, Eds., May 5-8, 2003 (Orlando, FL), ASM International, 2003, p 1591-1598
4. C.J. Li, W.B. Wang, A. Ohmori, and K. Tani, Relationship Between the Microstructure and Properties of Thermally Sprayed Deposits, *Proceedings of the 15th Thermal Spray Conference*, C. Coddet, Ed., May 25-29, 1998 (Nice, France), ASM International, **1**, p 481-487
5. C. Delbos, J. Fazilleau, V. Rat, J.F. Coudert, P. Fauchais, and B. Pateyron, Phenomena Involved in Suspension Plasma Spraying Part 2: Zirconia Particle Treatment and Coating Formation, *Plasma Chem. Plasma Process.*, 2006, **26**, p 393-414
6. P. Fauchais, V. Rat, C. Delbos, J.F. Coudert, T. Chartier, and L. Bianchi, Understanding of Suspension DC Plasma Spraying of Finely Structured Coatings for SOFC, *IEEE Trans. Plasma Sci.*, 2005, **33**, p 920-930
7. S. Deshpande, A. Kulkarni, S. Sampath, and H. Herman, Application of Image Analysis for Characterization of Porosity in Thermal Spray Coatings and Correlation with Small Angle Neutron Scattering, *Surf. Coat. Technol.*, 2004, **187**, p 6-16
8. C. Li and A. Ohmori, Relationship Between the Microstructure and Properties of Thermally Sprayed Deposits, *J. Therm. Spray Technol.*, 2002, **11**, p 365-374
9. F. Cernuschi, P. Bianchi, M. Leoni, and P. Scardi, Thermal Diffusivity/Microstructure Relationship in Y-PSZ Thermal Barrier Coatings, *J. Therm. Spray Technol.*, 1999, **8**, p 102-109
10. A.S. Houlbert, P. Cielo, C. Moreau, and M. Lamontagne, Measurement of Thermal Diffusivity and Anisotropy of Plasma-Sprayed Coatings, *Int. J. Thermophys.*, 1994, **15**, p 525-546
11. G.-E.-P Box, W.-G Hunter, and J.-S. Hunter, *Statistics for Experimenters an Introduction to Design, Data Analysis, and Model Buildings*. John Wiley & Sons Inc., Canada, 1978
12. J. Oberste Berghaus, J.G. Legoux, C. Moreau, F. Tarasi, and T. Chraska, Mechanical and Thermal Transport Properties of Suspension Thermal Sprayed Alumina-Zirconia Composite Coatings, *J. Therm. Spray Technol.*, 2008, **17**(1), p 91-104
13. U. Schulz, C. Leyens, K. Fritscher, M. Peters, B. Saruhan-Brings, and O. Lavigne, Some Recent Trends in Research and Technology of Advanced Thermal Barrier Coatings, *Aerosp. Sci. Technol.*, 2003, **7**, p 73-80
14. R. Soltani, T.W. Coyle, J. Mostaghimi, R.S. Lima, and C. Moreau, Thermo-Physical Properties of Plasma Sprayed Yttria Stabilized Zirconia Coatings, *Surf. Coat. Technol.*, 2008, **202**(16), p 3954-3959